

VOLTAGE DEPENDENT MODELS OF THE FORMATIVE TIME DELAY IN ARGON[†]

UDC 537.52:537.56

**Suzana N. Stamenković*, Vidosav Lj. Marković,
Aleksandar P. Jovanović, Marjan N. Stankov**

Department of Physics, Faculty of Sciences and Mathematics, University of Niš, Niš, Serbia

Abstract. *Measurements of the formative time delay t_f at different working voltages U in argon at low pressure are presented. The well-known decreasing voltage behavior of the formative time delay is theoretically described by different empirical and semi-empirical models. In addition to the introduced empirical models, some models from the literature are applied to elucidate experimentally obtained $t_f(U)$ dependence. However, the models from the literature show a good agreement with the experimental data only at low overvoltages ΔU ($\Delta U = U - U_s$, where U_s is the static breakdown voltage). Therefore, empirical corrections are made based on data analysis, and good compatibility is achieved in a whole range of working voltages.*

Key words: *argon discharge, electrical breakdown, formative time delay, empirical models, semi-empirical models*

1. INTRODUCTION

The study of electrical conductivity of gases is of importance for many applications in technology and different scientific areas: physics, electronics, engineering, medicine, etc. (Chapman, 1980; Druyvesteyn and Penning, 1940; Fridman, 2008; Lieberman and Lichtenberg, 1994; Makabe and Petrović, 2006; Mesyats, 2005; Raju, 2006; Zissis and Kitsinelis, 2009). However, under normal conditions, gases are not electrical conductors, but insulators. In order for them to become conductors, it is necessary to provide precisely determined conditions. Depending on the specific conditions, the electrical conductivity of gases, also known as electrical discharge, can be non-self-sustaining (maintenance of discharge due to the action of external factors – e.g. external sources of irradiation) and

Received: December 27th, 2017; accepted: January, 20th, 2018.

[†] Acknowledgement: The authors are grateful to the Ministry of Education, Science and Technological Development of the Republic of Serbia for the financial support (Project ON171025).

* **Corresponding author:** Suzana N. Stamenković

Department of Physics, Faculty of Science and Mathematics, Višegradska 3, 18000 Niš, Serbia

E-mail: ssuzana@pmf.ni.ac.rs

self-sustaining discharge (maintenance of discharge without activity of external elements) (Meek and Craggs, 1978; Raizer, 1991). The electrical breakdown of gases represents the process of their transition from a non-self-sustaining to a self-sustaining discharge. To enable this transition, it is necessary, among other things, to achieve a certain potential difference in gases, which is characterized by static breakdown voltage U_s , the lowest voltage which may cause a gas breakdown at given experimental conditions, providing the presence of the initiating electron(s) (Meek and Craggs, 1978; Raizer, 1991).

By connecting the voltage to the gas tube electrodes, there is no instantaneous transition from the non-self-sustaining to the self-sustaining discharge, but the electrical breakdown occurs with a certain delay, which is called time delay t_d . As the time between the moment of voltage application and the occurrence of breakdown, t_d consists of two separate periods, statistical t_s and formative t_f time delay, i.e. $t_d = t_s + t_f$. Statistical time delay is determined by the probability of the appearance of (a) successful initial electron(s) into the gap, while the formative time delay represent the time required for the development of discharge across the gap after it has been initiated (Meek and Craggs, 1978). The breakdown time delay depends on various factors such as inter-electrode distance d , the type of gas, the time interval τ between the application of the consecutive voltage signals (relaxation time), as well as the value of the operating voltage U itself. In order to better understand the physical processes that characterize this phenomenon, a simultaneous analysis of experimental results and theoretical models is required.

The first investigations of time delay voltage dependence date back to the end of the nineteenth century (Jaumann, 1895) when the shortening of the breakdown delay with increased voltage was determined. The decreasing of the formative time delay with growing overvoltage was confirmed by measurements in neon (Schade, 1937), while for a theoretical description, $t_f(U)$ dependence was derived that showed a good agreement with the experiment. (Druyvesteyn and Penning, 1940) derived a relation for the formative time delay voltage dependence based on the assumption that one ionization cycle is approximately equal to the transit time of an ion from the anode to the cathode and t_f consists of n ionization cycles. The formative time delay as a function of overvoltage has also been derived by (Raether, 1941a,b; Raether, 1949), taking into account not only the contribution of positive ions in the production of secondary electrons, but also the contribution of radiation from the gas. Therefore, in the derived relation, the electron transit time is present in addition to the ion transit time,. A theoretical analysis of the formative time delay measurements in the air at atmospheric pressure has been done by (Fletcher, 1949) based on the distribution of space charge in an avalanche and the assumption that formative time is the time taken for an avalanche to grow to a critical size (i.e. t_f is the rise time of the avalanche whose space charge field becomes comparable with the applied field). Another expression for the formative time voltage dependence at higher pressures is derived by (Kachickas and Fisher, 1952), using the assumption that the secondary electron emission occurs probably due to the photo-emission from the cathode. The derived expression shows a good agreement with the experimentally obtained t_f in the air, nitrogen and argon (Fisher and Bederson, 1951; Kachickas and Fisher, 1952; Kachickas and Fisher, 1953). The relations for the temporal growth of ionization currents, under constant potential difference in the absence of space charge distortion of the field, were used for the calculation of the formative time delay in different gases (Davidson, 1955; Dutton et al., 1953; Morgan, 1956). At the same time, by comparing the experimental

data and the theoretical analysis of ionization growth, the authors assessed the relative significance of possible secondary processes (Davidson, 1955; Dutton et al., 1953; Morgan, 1956).

The cited papers are only part of those related to the voltage dependence of the breakdown time delay. Some models are based on the Townsend's breakdown mechanism while others involve the streamer breakdown mechanism (Meek and Craggs, 1978). It is not possible to list all relevant papers, so only a few were mentioned.

In this paper, the measurements of the formative time delay, in argon at lower pressure (which provides Townsend's breakdown mechanism), as a function of overvoltage were analyzed and theoretically described by different empirical and semi-empirical models. The empirical models, expressed as power or exponential functions, are based on the experimentally obtained $t_f(U)$ dependence, which indicates a rapid decrease of the formative time with increasing the overvoltage. The semi-empirical models are based on the already existing models in the literature, but due to a certain deviation from the experimental data, empirical corrections were made.

2. EXPERIMENTAL DETAIL

For time delay measurements a gas tube made of borosilicate glass (8245, Schott technical glass) with a plane-parallel cylindrical oxygen-free high thermal conductivity (OFHC) copper cathode was used. The radius of the electrodes is $R = 1.1 \text{ cm}$ (front area $S = 3.8 \text{ cm}^2$) and both electrodes have slightly rounded edges in order to avoid edge effects and electric field inhomogeneity. Before the tube is filled with argon (Matheson Co. 99.9999% research purity argon with nitrogen impurity below 1 ppm) at the pressure of 200 Pa , the standard preparation procedure was carried out, which implies that the tube was evacuated down to the pressure of 10^{-5} Pa and baked at 600 K . The time delay measurements were carried out by applying a series of high-voltage rectangular ("step") voltage pulses to the tube, whereby one hundred single shots in a series per every working voltage U have been made. The time between the voltage pulses i.e. the afterglow period, was $\tau = 100 \text{ ms}$. The static breakdown voltage was $U_s \approx 240 \text{ V}$ (determined as the lowest working voltage in the measured $t_d(U)$ dependence), the inter-electrode distance $d = 15 \text{ mm}$, the glow current $I_g = 130 \mu\text{A}$ and the glow time $t_g = 1 \text{ s}$, long enough to establish steady-state glow discharge conditions. During the measurements, the tube was protected from the external light. More details about the experimental procedure, the measuring system and tube preparation can be found in Marković et al. (2005) and Stamenković et al. (2017).

3. EMPIRICAL MODELS OF THE FORMATIVE TIME DELAY

As stated in the introduction, this paper refers to the formative time delay voltage dependence in conditions of the Townsend's breakdown mechanism. The breakdown time delay measurements in specified conditions enable determination of the formative time delay in three different ways (Marković et al., 1997):

- from histograms as the minimum values of the breakdown time delay $t_f = t_{d\min}$;
- from a difference $t_f = \bar{t}_d - \bar{t}_s \approx \bar{t}_d - \sigma(t_d)$, taking into account the negligible fluctuation of the formative time delay $\sigma(t_f) \ll \sigma(t_s) \approx \sigma(t_d)$ and the fact that in given experimental conditions the standard deviation of the statistical time delay is approximately equal to its mean value $\sigma(t_s) \approx \bar{t}_s$;
- from the Laue diagrams by taking the t_f as the intersection values of the linear approximation of $\ln(n/N)$ (the measured data follow exponential distribution) with a time delay axis.

The selected experimental conditions lead to a good mutual agreement between the formative time delays obtained by using three indicated approaches. Afterwards, different empirical models were used to describe the formative time delay voltage dependence determined in this way.

The first applied empirical model given by relation:

$$t_f = \frac{c_1}{U - U_s}, \quad (1)$$

reflects a simple formative time delay voltage dependence $t_f \propto 1/\Delta U$ indicated by the previous studies (Gänger, 1953 Maier et al., 1993). The fit obtained with the empirical constant $c_1 = 11000 \mu sV$ and $U_s = 240V$, approximately equal to the static breakdown voltage, is presented in Fig. 1 by dashed line.

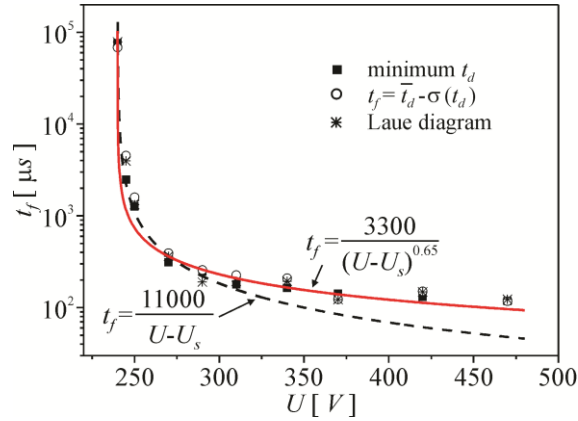


Fig. 1 Voltage dependence of the formative time delay: symbols – experimental data, dashed line – fit based on relation (1), red solid line – fit based on relation (2).

It is obvious that relation (1) shows a good agreement with the experimental data only at low overvoltage, and therefore its empirical improvement is made. In order to achieve a better agreement between the model and the experiment over the entire voltage range, a new empirical constant k is introduced into relation (1) that takes the form:

$$t_f = \frac{c_2}{(U - U_s)^k}. \quad (2)$$

The red solid line in Fig. 1 represents the fit obtained by relation (2) with $c_2 = 3300\mu sV^{0.65}$, $k = 0.65$ and $U_s = 240V$.

The next applied empirical model expresses the $t_f(U)$ dependence by introducing the voltage dependent electron ionization coefficient α (Meek and Craggs, 1978; Raizer, 1991) and its value α_s at the static breakdown voltage U_s :

$$t_f = \frac{c_3}{\alpha - \alpha_s}. \quad (3)$$

The coefficient α is given by the well-known Townsend semi-empirical relation:

$$\frac{\alpha}{p} = Ae^{-\frac{Bpd}{U}}, \quad (4)$$

where the parameter values $A = 10.87\text{ cm}^{-1}\text{ torr}^{-1}$ and $B = 174.56\text{ Vcm}^{-1}\text{ torr}^{-1}$ were obtained by fitting the experimental data from (Kruithof, 1940) for the range $U \approx (210 - 500)V$ covered in our experiment. The formative time delay fit based on relation (3) with the empirically determined constant $c_3 = 220\mu s\text{ cm}^{-1}$ and $\alpha_s = 3.17\text{ cm}^{-1}$ is presented by dashed lines in Fig. 2. The relation (3) describes the data well only for low overvoltage. Therefore, as in the case of the previous model, the empirical improvement is suggested in the form:

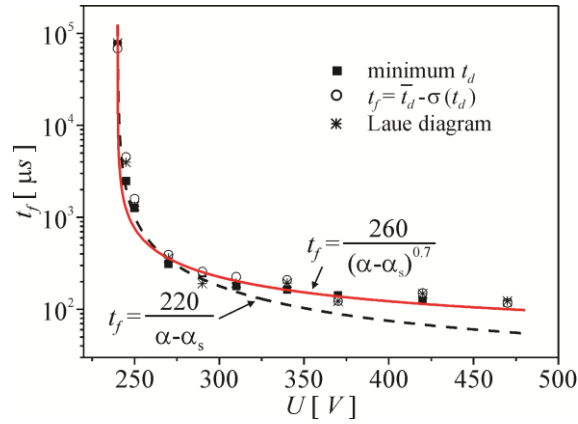


Fig. 2 Voltage dependence of the formative time delay: symbols – experimental data, dashed line – fit based on relation (3), red solid line – fit based on relation (5).

$$t_f = \frac{c_4}{(\alpha - \alpha_s)^k}. \quad (5)$$

The best agreement between the model and the experiment over the entire voltage range is obtained with $c_4 = 260\mu s\text{ cm}^{-0.7}$, $k = 0.7$, $\alpha_s = 3.17\text{ cm}^{-1}$ and the fit is shown by the red solid line in Fig. 2.

Other expressions based on power and exponential functions or their product, such as:

$$t_f = \frac{a_1}{U - U_{s1}} e^{-\frac{b_1}{U}}, \quad (6)$$

$$t_f = \frac{a_2}{U - U_{s2}} e^{b_2 U}, \quad (7)$$

$$t_f = a_3 e^{-\frac{b_3}{U - U_{s3}}}, \quad (8)$$

could be used for description of the formative time delay. These relations resemble the measured $t_f(U)$ dependence and by applying the appropriate values of the parameters a_i , b_i , U_{si} (Table 1), a good agreement with the experimental data is obtained (Fig. 3).

Table 1 The values of parameters in quoted relations

relation number	a_i	b_i	U_{si}
(6)	$10^5 \mu s V$	$620 V$	$240 V$
(7)	$4000 \mu s V$	$0.004 V^{-1}$	$240 V$
(8)	$110 \mu s$	$35 V$	$235 V$

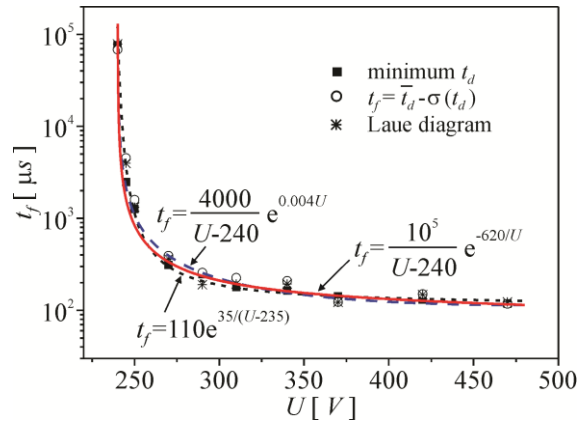


Fig. 3 Voltage dependence of the formative time delay: symbols – experimental data, red solid line – fit based on relation (6), blue dashed line – fit based on relation (7), dotted line – fit based on relation (8).

4. SEMIEMPIRICAL MODELS OF THE FORMATIVE TIME DELAY

The increase in the electron $n_e(t)$ and ion $n_i(t)$ number densities in the early stage of avalanche growth, in the approximation of negligible electron-ion recombination, can be obtained from the simple relation:

$$\frac{dn_e}{dt} = \frac{dn_i}{dt} = \alpha w_e n_e, \quad (9)$$

where α is the previously introduced Townsend's ionization coefficient and w_e electron drift velocity. In order to evaluate the ion number density, it is necessary to integrate this equation, whereby the assumption $n_e \approx n_i$ is accepted, as well as negligible space charge distortion of the electric field due to the early phase of avalanche growth. Taking into account the ion-electron emission from the cathode with the secondary electron yield γ_i (Meek and Craggs, 1978; Raizer, 1991), the boundary condition that connects the electron j_e and the ion j_i current density, takes the form:

$$j_e \approx \gamma j_i \Rightarrow n_e w_e \approx \gamma n_i w_i, \quad (10)$$

with w_i as the ion drift velocity. The voltage dependence of w_i is approximated by (Phelps and Petrović, 1999):

$$w_i = \frac{5.58 \frac{E}{N}}{\left[1 + \left(0.0077 \frac{E}{N}\right)^{1.68}\right]^{0.28}} \left[\frac{m}{s}\right], \quad (11)$$

based on the data from (von Engel, 1965) with the extrapolation to the values of the reduced field E/N (a ratio of the electric field and the gas density in the units of Townsend $1Td = 10^{-17} Vcm^{-2}$) from the experiment. In addition, we took into account the domination of the molecular Ar_2^+ ions due to the atomic-molecular ion conversion in the first few millisecond of the afterglow (Marković et al., 2005). When the general solution is subject to boundary and initial conditions on the cathode, the outcome is a temporal evolution of the ion number density:

$$n_i \approx n_{i0} e^{\alpha \gamma w_i t}, \quad (12)$$

where n_{i0} is the initial ion number density. According to (12), the ion number density n_{it} , which corresponds to the transition from negligible to non-negligible space charge and the electric field distortion (Marković et al., 2007), can be written as:

$$n_{it} \approx n_{i0} e^{\alpha \gamma w_i t_f}, \quad (13)$$

which enables the expression of the formative time delay:

$$t_f = \frac{1}{\alpha \gamma w_i} \ln \frac{n_{it}}{n_{i0}}. \quad (14)$$

The value of the ion number density $n_{it} \approx I_{it} / e w_i S \approx 1.47 \cdot 10^7 cm^{-3}$ used for the modeling of experimental $t_f(U)$ dependence, is based on the current in the Townsend's dark discharge $I_{it} = 1 \mu A$. This value is obtained from the $I-U$ characteristic as the current before the collapse of the applied voltage (indicated in Fig. 4), while the initial ion number density $n_{i0} = 5 \cdot 10^6 cm^{-3}$ is determined as a fitting parameter. The electric field

distortion by non-negligible space charge in the later stages of avalanche growth leads to rapid changes in the current and voltage. However, the fast current rise time is of the order of several microseconds and its contribution to the t_f could be neglected (Marković et al., 2007).

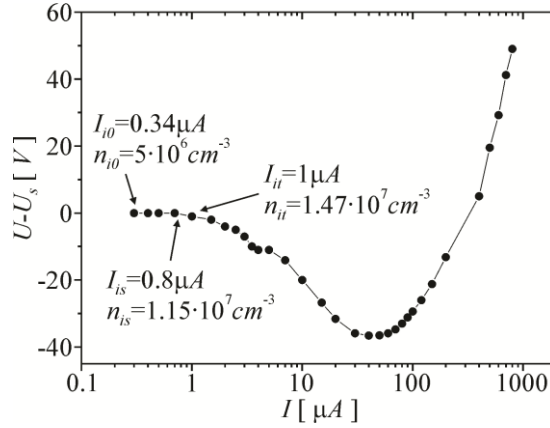


Fig. 4 The $I - U$ characteristic at inter-electrode distance $d = 15 \text{ mm}$ with marked Townsend's dark discharge current I_{ii} before collapse of the applied voltage and the corresponding ion number density n_{ii} .

The best fit of formative time delay data with specified ion number densities and the secondary electron yield $\gamma = 8.6 \cdot 10^{-3}$, corresponding to the static breakdown voltage $U_s = 240 \text{ V}$, is shown in Fig. 5 by dashed lines. It is obvious that this model, expressed by relation (14), fits the data only at high overvoltage and cannot describe the formative time singularity at working voltage near the U_s . The introduction of singularity $t_f \rightarrow \infty$ at $U \rightarrow U_s$ into the previous model is possible by defining the ion number density n_{is} as an approximate pre-ionization level at the static breakdown voltage:

$$n_{is} \approx n_{i0} e^{\alpha_s \gamma w_i t_f}, \quad (15)$$

with the corresponding ionization coefficient α_s . From the relations (13) and (15) it follows:

$$n_{ii} \approx n_{is} e^{(\alpha - \alpha_s) \gamma w_i t_f}. \quad (16)$$

Thus, the formative time delay with singularity at $U \rightarrow U_s$ (i.e. $\alpha \rightarrow \alpha_s$) is obtained in the form:

$$t_f \approx \frac{1}{(\alpha - \alpha_s) \gamma w_i} \ln \frac{n_{ii}}{n_{is}}. \quad (17)$$

The best fit (that achieves agreement with the experiment over the entire voltage range) based on the previous relation with the fitting parameter $n_{is} = 1.15 \cdot 10^7 \text{ cm}^{-3}$ and decreasing γ from the interval (0.011 – 0.003) is shown in Fig. 5 by a red solid line.

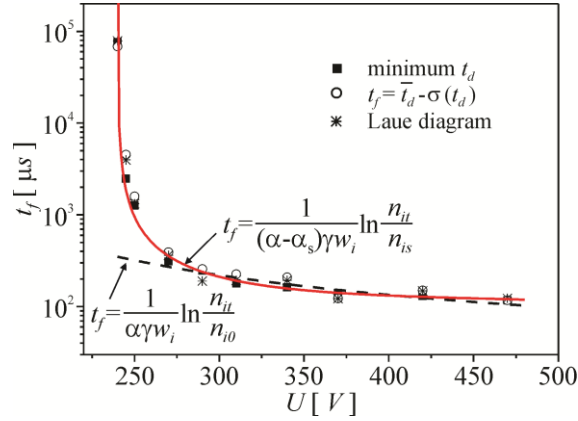


Fig. 5 Voltage dependence of the formative time delay: symbols – experimental data, red solid line – fit based on relation (17), dashed line – fit based on relation (14).

4.1. Schade's model

The Schade's model (Schade, 1937) relates the formative time delay at low gas pressures with the voltage applied to the gap, taking into account that t_f corresponds to the time of positive ions movements across the gap (assuming that cathode bombardment by positive ions is the main mechanism of the secondary emission). The derived expression:

$$t_f = \frac{a(U)}{U - U_s} e^{-\frac{b}{U}} \quad (18)$$

contains two parameters, the one

$$a(U) = \frac{U_s^2}{ABp^2 d w_i} \ln \left[1 + \frac{I}{I_0} \frac{(U - U_s)}{U_s^2} ABp^2 d^2 e^{-\frac{Bpd}{U}} \right] \quad (19)$$

that is voltage-dependent and the other $b = Bpd$ whose value does not change with voltage. Taking the required data from the experimental conditions, from the relation (4) and the current ratio $I/I_0 = 10^{10}$ as suggested in (Schade, 1937), the parameters get the values: $a \approx (1381 - 1735) \mu s V$, $b = 392.8 V$. The fit using the obtained values is shown in Fig. 6a, by the black dashed line, while $a(U)$ dependence based on Schade' model is presented in Fig. 6b, by the same dashed line. According to Fig. 6a, it follows that this model describes the experimental formative time delay only at low overvoltage. A similar result is obtained by applying a constant value for the parameter $a = 2500 \mu s V$ (blue dotted line in Fig. 6b) and $b = 392.8 V$, while the corresponding fit of $t_f(U)$ is shown in Fig. 6a by the blue dotted line.

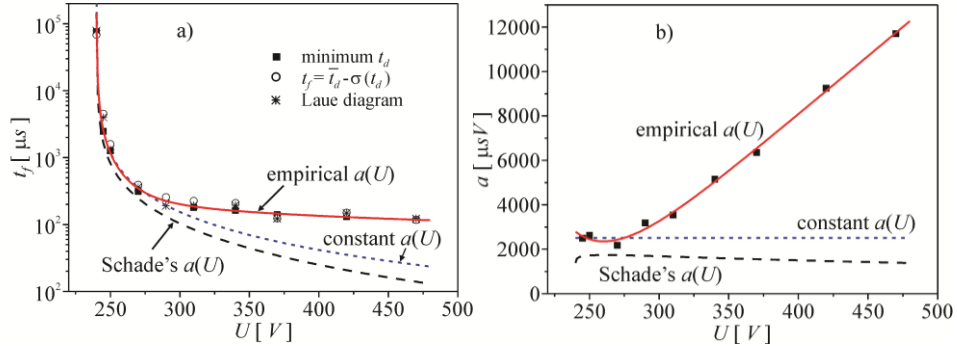


Fig. 6 a) Voltage dependence of the formative time delay: symbols – experimental data, dashed line – fit with $a(U)$ expressed by relation (19) based on the model from (Schade, 1937), blue dotted line – fit with the constant parameter a , red solid line – fit with the empirical $a(U)$ expressed by relation (20); b) The $a(U)$ dependence: dashed line – relation (19) based on the model from (Schade, 1937), blue dotted line – constant a , symbols – empirically obtained a , red solid line – empirical $a(U)$ expressed by relation (20).

Due to the apparent deviation of Schade's model at high overvoltage, an empirical correction of the parameter $a(U)$ was made to achieve an agreement with the experiment over the entire range of the applied voltages and the result is presented by symbols (■) in Fig. 6b. The empirically obtained dependence could be described by the relation:

$$a(U) = 7.52 \cdot 10^6 e^{-0.032U} - 12926.3 + 52.5U \text{ } [\mu s V], \quad (20)$$

that indicates exponential decreasing of a at low overvoltage and linear increasing at high overvoltage (the red solid line in Fig. 6b). The fit of the formative time with the empirical $a(U)$, given by relation (20), is shown in Fig. 6a by the red solid line.

4.2. Davidson's model

Davidson's model is based on ionization current growth in a uniform electric field (constant potential difference between parallel electrodes) with secondary electron generation due to the action of photons and positive ions on the cathode. It was shown that the same primary and secondary ionization processes, which lead to the pre-breakdown current growth, also lead to the rapid formative time delay decreasing (Davidson, 1955; Dutton et al., 1953; Morgan, 1956). Adopting the model to our experimental conditions (negligible photon contribution), the electron and ion currents growth at large t have the form:

$$i_-(t) = A - B e^{\lambda(U)t}, \quad (21)$$

$$i_+(t) = \int_0^d \alpha i_-(t - \frac{x'}{w}) e^{\alpha x'} dx', \quad (22)$$

where A and B are constants and drift velocity w , determined from the electron and ion drift velocities as $1/w = 1/w_e + 1/w_i$, is approximately equal to w_i because of $w_e \gg w_i$. The growth parameter $\lambda(U)$ present in (21) is obtained as the real root of the characteristic equation:

$$\gamma \frac{\alpha}{\alpha - \lambda/w_i} [e^{(\alpha - \lambda/w_i)d} - 1] = 1, \quad (23)$$

which also is modified according to the fact that the secondary electron emission by positive ions is a predominant process on the cathode. The temporal growth of the ion current, with appropriate initial and boundary conditions (Davidson, 1955; Dutton et al., 1953; Morgan, 1956), enables the derivation of the formative time delay expression in the form:

$$t_f = \frac{1}{\lambda} \ln \left\{ \frac{\alpha - \lambda/w_i}{\alpha} \left[e^{\alpha d} - 1 - (1-q) \frac{i_+}{i_0} \right] \left[e^{(\alpha - \lambda/w_i)d} - 1 \right]^{-1} \right\}. \quad (24)$$

The best fit of the experimental $t_f(U)$ dependence using relation (24) with the implementation of (23) and the fitting parameter $i_+/i_0 = 10^{15}$ is shown in Fig. 7a, by a dashed line. The corresponding growth parameter λ is presented by the open triangle symbol in Fig. 7b, showing the linear voltage dependence (dashed line in Fig. 7b).

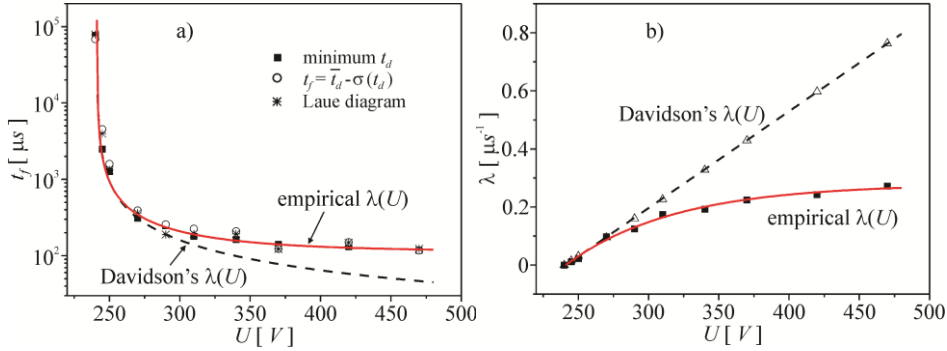


Fig. 7 a) Voltage dependence of the formative time delay: symbols – experimental data, dashed line – fit with $\lambda(U)$ obtained from relation (23) based on Davidson's model, red solid line – fit with the empirical $\lambda(U)$ given by (25); b) The $\lambda(U)$ dependence: open triangles and dashed line – $\lambda(U)$ as suggested in (Davidson, 1955; Dutton et al., 1953; Morgan, 1956), squares and red solid line – empirically obtained $\lambda(U)$ expressed by relation (25).

As in the case of Schade's model, the agreement of Davidson's model (24) with the experiment is achieved only at low overvoltage. Accordingly, an empirical correction of the parameter $\lambda(U)$ was made, thus improving the agreement of the model and the experiment throughout the voltage range. The fit including our empirical dependence:

$$\lambda(U) = 0.28 - 0.28e^{-(U-240)/77.8} [\mu\text{s}^{-1}] \quad (25)$$

and the fitting parameter $i_+ / i_0 = 10^{15}$ is shown in Fig. 7a by the red solid line. The corresponding empirically obtained values of λ are shown in Fig. 7b (■) accompanied by dependence (25) (the red solid line in Fig. 7b).

5. CONCLUSION

Several approximate empirical and semi-empirical models are applied for description of decreasing behavior of the formative time delay voltage dependence in argon at low pressures. Different models show a different agreement with the experimental data, depending on whether they are based on power, exponential functions or the product of power and exponential functions. Also, the models from the literature are used for description of $t_f(U)$ dependence, but the applied models achieve a good agreement with the experimental data only at low overvoltage. Because of their deviation at high working voltage, certain corrections are necessary. In this paper, empirical corrections of the existing models are suggested, thus achieving an excellent agreement with the experiment over the entire voltage range. The application of appropriate, theoretically founded simple models allows for a better understanding of the basic physical processes in various experiments. Consequently, a simultaneous analysis of the experimental results and theoretical models could be useful for studying the formative time delay under different conditions.

REFERENCES

- Chapman, B.N., 1980. Glow discharge processes: sputtering and plasma etching, John Wiley and Sons, New York.
- Davidson, P.M., 1955. Phys. Rev. 99, 1072-1974. DOI:https://doi.org/10.1103/PhysRev.99.1072
- Druyvesteyn, M.J., Penning, F.M., 1940. Rev. Mod. Phys., 12, 87-174.
DOI:https://doi.org/10.1103/RevModPhys.12.87
- Dutton, J., Haydon, S.C., Jones, F.L., with mathematical appendix by P.M. Davidson, 1953. Brit. J. Appl. Phys. 4, 170-175. DOI:https://doi.org/10.1088/0508-3443/4/6/303
- Fisher, L.H., Bederson B., 1951. Phys. Rev. 81, 109-114. DOI:https://doi.org/10.1103/PhysRev.81.109
- Fletcher, R.C., 1949. Phys. Rev. 76, 1501-1511. DOI:https://doi.org/10.1103/PhysRev.76.1501
- Fridman, A., 2008. Plasma chemistry, Cambridge University Press, Cambridge, New York.
- Gänger, B., 1953. Der elektrische Durchschlag von Gasen, Springer-Verlag, Berlin.
- Jaumann G., 1895. Ann. Phys. (Leipzig), 291, 656-683. DOI:10.1002/andp.18952910811
- Kachickas, G.A., Fisher, L.H., 1952. Phys. Rev. 88, 878-883.
DOI:https://doi.org/10.1103/PhysRev.88.878
- Kachickas, G.A., Fisher, L.H., 1953. Phys. Rev. 91, 775-779.
DOI:https://doi.org/10.1103/PhysRev.91.775
- Kruithof, A.A., 1940. Physica, 7, 519-540. DOI:https://doi.org/10.1016/S0031-8914(40)90043-X
- Lieberman, M.A., Lichtenberg, A.J., 1994. Principles of Plasma Discharges and Material Processing, John Willey & Sons, New York.
- Maier, W.B., Kadish, A., Buchenauer, C.J., Robiscoe, R.T., 1993. IEEE Transactions on plasma science, 21, 676-683. DOI:10.1109/27.256787
- Makabe, T., Petrović, Z.Lj., 2006. Plasma Electronics: Applications in Microelectronic Device Fabrication, CRC Press, Taylor & Francis Group, New York.

- Marković, V.Lj., Petrović, Z.Lj., Pejović, M.M., 1997. Plasma Sources Sci. Technol. 6, 240-246. DOI:https://doi.org/10.1088/0963-0252/6/2/018
- Marković, V.Lj., Gocić, S.R., Stamenković, S.N., Petrović, Z.Lj., 2005. Physics of plasmas, 12, 073502-1-8. DOI:http://aip.scitation.org/doi/10.1063/1.1942499
- Marković, V.Lj., Stamenković, S.N., Gocić, S.R., 2007. Contrib. Plasma Phys., 47, 413-420. DOI: 10.1002/ctpp.200710054
- Meek, J.M., Craggs, J.D., (Eds.), 1978. Electrical Breakdown of Gases, John Wiley & Sons, Chichester, pp. 655-688.
- Mesyats, G.A., 2005. Pulsed Power, Springer, New York.
- Morgan, C.G., 1956. Phys. Rev. 104, 566-571. DOI:https://doi.org/10.1103/PhysRev.104.566
- Phelps, A.V., Petrović, Z.Lj., 1999, Plasma Sources Sci. Technol. 8, R21-R44. DOI:https://doi.org/10.1088/0963-0252/8/3/201
- Raether, H., 1941.a Z. Phys, 117, 375-398. DOI:https://doi.org/10.1007/BF01676336
- Raether, H., 1941.b Z. Phys. 117, 524-542. DOI:https://doi.org/10.1007/BF01668950
- Raether H., 1949. Die Entwicklung der Elektronenlawine in den Funkenkanal. In: Flüge S., Trendelenburg F. (eds) Ergebnisse der Exakten Naturwissenschaften. Ergebnisse der Exakten Naturwissenschaften, vol 22. Springer, Berlin, Heidelberg. DOI:https://doi.org/10.1007/978-3-662-25834-7_3
- Raizer, Yu.P., 1991. Gas discharge physics, Springer-Verlag, Berlin.
- Raju, G.G., 2006. Gaseous electronics: theory and practice, CRC Press, Taylor & Francis Group, Boca Raton.
- Schade, R., 1937. Z. Phys. 104, 487-510. DOI:https://doi.org/10.1007/BF01330065
- Stamenković, S.N., Marković, V.Lj., Jovanović, A.P., Stankov, M.N., 2017. Romanian reports in physics, 69, 408-1-16.
- von Engel A., 1965. Ionized Gases, Clarendon Press, Oxford
- Zissis, G., Kitsinelis, S., 2009. J. Phys. D: Appl. Phys., 42, 173001. DOI:https://doi.org/10.1088/0022-3727/42/17/173001

NAPONSKI ZAVISNI MODELI VREMENA FORMIRANJA PRAŽNENJA U ARGONU

U radu su prikazana merenja vremena formiranja pražnjenja t_f u argonu, pri niskim pritiscima i na različitim radnim naponima U . Opadanje vremena formiranja pražnjenja sa porastom napona teorijski je opisano različitim empirijskim i semiempirijskim modelima. Takođe, postojeći modeli iz literature primenjeni su za opisivanje eksperimentalno dobijene zavisnosti $t_f(U)$. Međutim, modeli iz literature pokazuju slaganje sa eksperimentom samo na niskim prenaponima ΔU ($\Delta U = U - U_s$ gde je U_s statički probojni napon). Na osnovu analize eksperimentalnih podataka urađene su empiriske korekcije postojećih modela i na taj način postignuto je dobro slaganje sa eksperimentom u celokupnom opsegu radnih napona.

Ključne reči: pražnjenje u argonu, električni proboj, vreme formiranja pražnjenja, empirijski modeli, semiempirijski modeli